

New estimate of the chromomagnetic dipole moment of quarks in the standard model

A. I. Hernández-Juárez ^{a,1}, A. Moyotl ^{b,2}, G. Tavares-Velasco ^{c,1}

¹Facultad de Ciencias Físico-Matemáticas,
Benemérita Universidad Autónoma de Puebla,
C.P. 72570, Puebla, Pue., Mexico

²Ingeniería en Mecatrónica,
Universidad Politécnica de Puebla,
Tercer Carril del Ejido Serrano s/n, San Mateo Cuanalá, Juan C. Bonilla,
Puebla, Puebla, México

Received: date / Accepted: date

Abstract A new estimate of the one loop contributions of the standard model to the chromomagnetic dipole moment (CMDM) $\hat{\mu}_q$ of quarks is presented with the aim to address a few disagreements arising in previous calculations. We consider the most general case with non-zero gluon transfer momentum q^2 and obtain analytical results in terms of Feynman parameter integrals and Passarino-Veltman scalar functions, which are then expressed in terms of closed form functions when possible. It is found that the QCD contribution from a three-gluon Feynman diagram diverges at $q^2 = 0$, which agrees with a previous evaluation and stems from the fact that the static CMDM $[\hat{\mu}(0)]$ has no sense in perturbative QCD. For the numerical analysis we consider the region $30 \text{ GeV} < \|q\| < 1000 \text{ GeV}$ and analyze the behavior of $\hat{\mu}_q(q^2)$ for all the SM quarks. It is found that the CMDM of light quarks is considerably smaller than that of the top quark as it is directly proportional to the quark mass. In the considered energy interval, both the real and imaginary parts of $\hat{\mu}_t(q^2)$ are of the order of $10^{-2} - 10^{-3}$, with the largest contribution arising from the QCD induced diagrams, though around the threshold $q^2 = 4m_t^2$ there are also important contributions from diagrams with Z gauge boson and Higgs boson exchange.

Keywords Top quark · Chromomagnetic dipole moments · Standard model

^aalaban7_3@hotmail.com

^bagustin.moyotl@uppuebla.edu.mx

^cgtv@cfm.buap.mx

1 Introduction

The anomalous magnetic dipole moment (MDM) of fermions has been a fertile field of study, giving rise to a plethora of theoretical work within the context of the standard model (SM) [1, 2, 3, 4], as well as beyond the SM (BSM) theories [5]. Furthermore, the fermion electric dipole moment (EDM) has also been analyzed in several models [6, 7, 8, 9, 10, 11]. More recently, the calculation of radiative corrections to the gluon-quark-quark $\bar{q}qg$ vertex has also become a topic of considerable interest. Radiative corrections to the $\bar{t}tg$ coupling are expected to be considerably larger than those of lighter quarks due to the large top quark mass [12]. In particular the top quark chromomagnetic dipole moment (CMDM) and chromoelectric dipole moment (CEDM) have been studied within the framework of the SM [13], two-Higgs doublet models (THDMs) [14], the four-generation THDM (4GTHDM) [12], models with heavy Z gauge bosons [15], little Higgs models [16, 17], the minimal supersymmetric standard model (MSSM) [18], unparticle model [19], vector like multiplet models [20], etc.

The anomalous $\bar{q}qg$ coupling can be written as

$$\mathcal{L} = \frac{g_s}{2} \bar{q} T^a \sigma_{\mu\nu} \left(\frac{a_q}{2m_q} + i d_q \gamma^5 \right) q G_a^{\mu\nu}, \quad (1)$$

where a_q and d_q are the CMDM and CEDM, respectively, whereas $G_a^{\mu\nu}$ is the gluon stress tensor and T^a are the $SU(3)$ color generators. The CMDM and CEDM are usually defined in the literature as dimensionless parameters [21]

$$\hat{\mu}_q(\hat{d}_q) \equiv \frac{m_q}{g_s} \mu_q(d_q), \quad (2)$$

where $\hat{\mu}_q = a_q/2$ and $\hat{d}_q = m_q d_q$. In the case of the quark top, the most recent experimental bounds from CMS are $-0.014 < \hat{\mu}_t < 0.004$ and $-0.020 < \hat{d}_t < 0.012$ [22].

In the SM, the CMDM is induced at the one-loop level or higher orders via electroweak (EW) and QCD contributions depicted in Figs. 1 and 2, respectively. On the other hand, the CEDM is induced up to the three-loop level [23, 24] since all the partial contributions exactly cancel out at the two-loop level [25]. The lowest order SM contributions to the CMDM of the top quark have been studied in [13] and more recently in [26, 15]. However, there are some disagreement between those calculations (see section 2.1 of [26] and section 3.D of [15]). In particular, authors of Ref. [13] only focus on the static CMDM, which they claim it receives a finite QCD contribution, whereas authors of Ref. [26] argue that the on-shell CMDM has no sense in perturbative QCD as the contribution arising from the three-gluon vertex diagram of Fig. 2 diverge, so they extend the analysis to the off-shell CMDM. Even more, the analytical results presented in [13], [26] and [15] disagree. In the experimental side, the advent of the LHC has triggered the interest on the anomalous $\bar{t}t g$ couplings, which have become an interesting area of study in experimental particle physics. Searches for any deviation to the SM $\bar{t}t$ production has made it possible to set constraints on the top quark CMDM and CEDM, which are regularly improved [27, 21, 22]. In fact, the current upper bounds [22] have been improved by one order of magnitude as compared to the previous ones [21]. Hopefully, more tight constraints on these top quark properties, closer to the SM predictions, would be achieved in the future, and thus a more precise and unambiguous prediction of the SM contributions to the top quark CMDM is mandatory. Also, since contributions to the CMDM in extension theories could give rise to an important enhancement, a precise determination of such contributions is in order.

In this work we present a new calculation of the SM contributions to the quark CMDM, which is aimed to address some ambiguities of previous results. Our manuscript is organized as follows. In Sec. 2, we present the main steps of the analytical calculation, stressing any disagreement with previous results. The corresponding loop functions are presented in terms of Feynman parameter integrals, Passarino-Veltman scalar functions and closed form results in Appendix Appendix A, which may be useful for a numerical cross-check. In Sec. 3, we present a numerical analysis and discussion of the behavior of the CMDM of SM quarks, with emphasis on the top quark one. The conclusions are presented in Sec. 4.

2 Analytical results

The CMDM is defined in a similar fashion to the electromagnetic case. We thus write the S -matrix element for $\bar{q}qg$ coupling as

$$i\mathcal{M} = ig_s T^a \bar{u}(p_2) \Gamma^\mu u(p_1), \quad (3)$$

where, from Lagrangian 1, the corresponding vertex function Γ^μ can be written as

$$\Gamma^\mu = i\sigma_{\mu\nu} q^\nu \left(\frac{a_q}{2m_q} + id_q \gamma^5 \right). \quad (4)$$

We now turn to outline the main steps of the calculation. For completeness, the loop functions are presented in terms of Feynman parameter integrals, Passarino-Veltman scalar functions, and closed form functions, which can be useful for a numerical cross-check. The Dirac algebra and tensor reduction was done with the help of FeynCalc [28] and Package-X [29].

Below, p_1 (p_2) denotes for the four-momentum of the ingoing (outgoing) quark, whereas q is the gluon four-momentum. We first present the calculation of the QCD contributions arising from the Feynman diagrams of Fig. 2, which are then compared with previous results. Afterwards the calculation of the EW contributions from the Feynman diagrams of Fig. 1 is presented.

2.1 QCD contribution

The contribution to the vertex function Γ^μ from diagram 2(a) is

$$\Gamma_{\text{QCD}_1}^\mu = \frac{ig_s^2}{6} \int \frac{d^D \hat{k}}{(2\pi)^D} \frac{\gamma^\beta (\not{q}_2 + m_q) \gamma^\mu (\not{q}_1 + m_q) \gamma_\beta}{(q_2^2 - m_q^2) (q_1^2 - m_q^2) (k^2)}, \quad (5)$$

where $q_i = k + p_i$, and m_q is the quark mass. Also $d^D \hat{k} = \mu^{4-D} d^D k$, with μ the scale of dimensional regularization, and it is understood that a small imaginary part $i\epsilon$ is added to the propagators. In this case we have three color generators T^a , which simplifies as follows

$$T_{jn}^b T_{nm}^a T_{mi}^b = \frac{1}{2} \delta_{ji} T_{nn}^a - \frac{1}{2N} T_{ji}^a = -\frac{1}{6} T_{ji}^a, \quad (6)$$

where we used $T_{jn}^b T_{mi}^b = \frac{1}{2} (\delta_{ji} \delta_{nm} - \frac{1}{N} \delta_{jn} \delta_{mi})$ and $\text{Tr}[T^a] = 0$, whereas N stands for the quark color number. After Feynman-parameter integration, the following contribution to the CMDM is obtained:

$$a_q^{\text{QCD}_1}(q^2) = \frac{\alpha_s}{6\pi} \mathcal{F}_q^{\text{QCD}_1}(q^2), \quad (7)$$

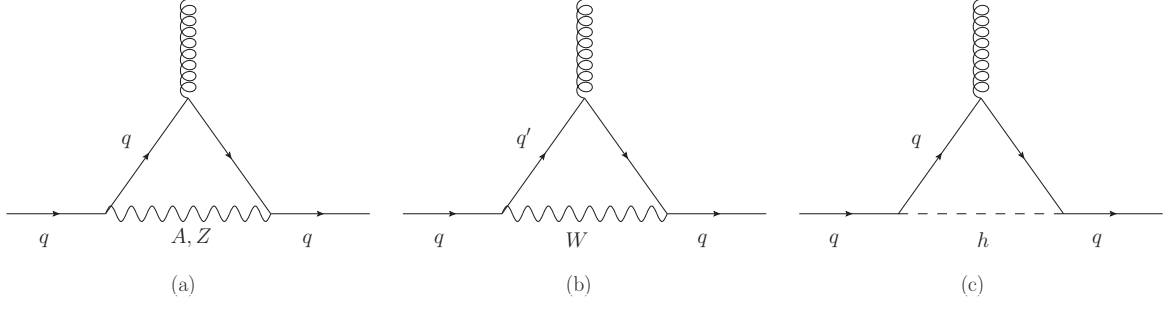


Fig. 1 One-loop Feynman diagrams for the electroweak contributions to the CMDM of quarks at the one-loop level in the SM: (a) and (b) gauge boson exchange and (c) Higgs boson exchange.

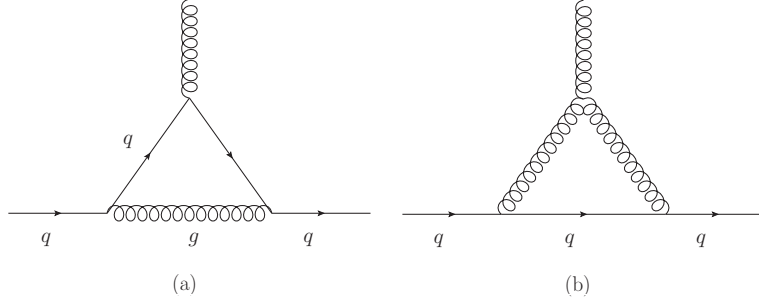


Fig. 2 One-loop Feynman diagrams for the QCD contributions to the CMDM of quarks: (a) QED-like diagram and (b) three-gluon diagram.

where the function $\mathcal{F}_q^{\text{QCD}_1}$ is presented in Appendix A.1. When $q^2 = 0$, it is straightforward to obtain

$$a_q^{\text{QCD}_1}(0) = -\frac{\alpha_s}{12\pi}, \quad (8)$$

which agrees with the well-known QED result after the replacement of the electric charge e by the strong coupling constant α_s and the color factor of Eq. (6).

The non-abelian contribution to the quark CMDM from diagram 2(a) can be obtained from the vertex function:

$$\Gamma_{\text{QCD}_2}^\mu = -\frac{i3g_s^2}{2} \int \frac{d^D k}{(2\pi)^D} \frac{\gamma_\beta (-\not{k} + m_q) \gamma_\alpha \Sigma^{\alpha\beta\mu}(k)}{(q_2^2)(k^2 - m_q^2)(q_1^2)}, \quad (9)$$

with

$$\Sigma^{\alpha\beta\mu}(k) = g^{\alpha\beta} (p_1 + p_2 + 2k)^\mu + g^{\beta\mu} (-2p_2 + p_1 - k)^\alpha + g^{\mu\alpha} (p_2 - k - 2p_1)^\beta, \quad (10)$$

¹From now on, all the corresponding loop functions appearing in the contributions to $a_q(q^2)$, denoted by calligraphy letters, will be presented in terms of Feynman parameter integrals, Passarino-Veltman scalar functions and closed form results in appendices A.1, A.2, and A.3, respectively, including the results for $q^2 = 0$.

and the color factor can be worked out as follows

$$T_{jb}^m T_{bi}^n f^{anm} = -2i \text{Tr} [T^m [T^n, T^a]] T_{jb}^m T_{bi}^n = -\frac{i3}{2} T_{ji}^a. \quad (11)$$

After four-momentum integration, our result for the quark CMDM is given as

$$a_q^{\text{QCD}_2}(q^2) = \frac{3\alpha_s}{2\pi} \mathcal{F}_q^{\text{QCD}_2}(q^2), \quad (12)$$

which disagrees with the result obtained in [26] as there is a disagreement with the color factor used by those authors.

When $q^2 = 0$, Eq. (12) yields a divergent result for $q^2 = 0$:

$$\begin{aligned} \mathcal{F}_q^{\text{QCD}_2}(0) &= \frac{1}{2} (\mathbf{B}_0(0; m_q, m_q) + 3) \\ &= \frac{1}{2} \left(\frac{1}{\epsilon} + \log \left(\frac{\mu^2}{m_q^2} \right) + 3 \right), \end{aligned} \quad (13)$$

where $\mathbf{B}_0(0; m_q, m_q)$ is a two-point Passarino-Veltman scalar function and ϵ is the pole of dimensional regularization. Therefore, the contribution of the three-gluon diagram is not well defined when $q^2 = 0$ as it was also pointed out in [26]. Since QCD contributions to the CMDM are proportional to the strong running coupling

constant $\alpha_s(q^2)$, such contributions have not perturbative sense at $q^2 = 0$ but at scales where perturbative calculations are allowed. We also performed the numerical calculation of the QCD contributions to the CMDM using a small fictitious mass for the internal gluon. The numerical evaluation shows little dependence on this fictitious gluon mass.

2.2 Electroweak contribution

We now present the calculation of the contributions to the quark CMDM induced through the Feynman diagrams of Fig. 1. We note that the diagrams with photon, Z gauge boson, and Higgs boson exchange are similar to those inducing a lepton anomalous MDM [2], but with the external photon replaced by a gluon. Therefore, the corresponding S-matrix elements of the couplings $\bar{q}q\gamma$ and $\bar{q}qg$ just differ by the coupling constants g_s instead of the electric charge and the $SU(3)$ generators T_{ij}^a , although the vertex function is the same in both cases. Then, the results for the CMDM must reproduce the lepton anomalous MDM ones. As far as the diagram with W^\pm gauge boson exchange is concerned, the lepton anomalous MDM has no analogous contribution in the SM.

2.2.1 Photon exchange

The corresponding contribution to the $\bar{q}qg$ vertex function can be written as

$$\Gamma_A^\mu = -ie^2 Q_q^2 \int \frac{d^D k}{(2\pi)^D} \frac{\gamma^\beta (q_2 + m_q) \gamma^\mu (q_1 + m_q) \gamma_\beta}{(q_2^2 - m_q^2) (q_1^2 - m_q^2) (k^2)}, \quad (14)$$

with Q_q the quark electric charge in units of e . After a straightforward calculation, we arrive at the following expression

$$a_q^A(q^2) = -\frac{e^2 Q_q^2}{4\pi^2} \mathcal{F}_q^A(q^2), \quad (15)$$

which gives a result similar to that of the lepton anomalous MDM for $q^2 = 0$:

$$a_q^A(0) = \frac{\alpha Q_q^2}{2\pi}. \quad (16)$$

We note that the electric charge factor Q_q^2 is missing in the corresponding result of [26]. However, since the internal photon of diagram 1(a) is attached to two quark lines, such a factor do appear in this contribution.

2.2.2 Z gauge boson exchange

The contribution of the loop with Z gauge boson exchange to the $\bar{q}qg$ vertex function in terms of the axial (vector) g_A^q (g_V^q) couplings is:

$$\Gamma_Z^\mu = \frac{-ig^2}{c_W^2} \int \frac{d^D k}{(2\pi)^D} \frac{\Xi^\mu}{(q_2^2 - m_q^2) (q_1^2 - m_q^2) (k^2 - m_Z^2)}, \quad (17)$$

where

$$\begin{aligned} \Xi^\mu &= \gamma^\beta (g_V^q - g_A^q \gamma^5) (q_2 + m_q) \gamma^\mu (q_1 + m_q) \gamma^\lambda \\ &\times (g_V^q - g_A^q \gamma^5) \left(g_{\beta\lambda} - \frac{k_\beta k_\lambda}{m_Z^2} \right) \end{aligned} \quad (18)$$

After integration in the four-momentum space we obtain

$$a_q^Z(q^2) = \frac{\sqrt{2} G_F m_q^2}{\pi^2} \left((g_A^q)^2 \mathcal{A}_q^Z(q^2) + (g_V^q)^2 \mathcal{V}_q^Z(q^2) \right), \quad (19)$$

whereas the result obtained for $q^2 = 0$ is analogue to Eq. (3) of [2] for the contribution of the lepton anomalous MDM. There is agreement with the calculation presented in [15], but there is no agreement with the result of [26] as those authors perform the calculation in the Feynman-'t Hooft gauge.

2.2.3 W^\pm gauge boson exchange

We now calculate the contribution from the Feynman diagram of Fig. 1(b). The $\bar{q}qg$ vertex function can be written as

$$\begin{aligned} \Gamma_W^\mu &= \sum_{q'} \frac{-ig^2 |V_{qq'}|^2}{8} \int \frac{\mu^{4-D} d^D k}{(2\pi)^D} \Pi^\mu \\ &\times \frac{1}{(q_2^2 - m_{q'}^2) (q_1^2 - m_{q'}^2) (k^2 - m_W^2)}, \end{aligned} \quad (20)$$

with

$$\begin{aligned} \Pi^\mu &= \gamma^\beta (1 - \gamma^5) (q_2 + m_{q'}) \gamma^\mu (q_1 + m_{q'}) \gamma^\lambda (1 - \gamma^5) \\ &\times \left(g_{\beta\lambda} - \frac{k_\beta k_\lambda}{m_W^2} \right) \end{aligned} \quad (21)$$

where q' stands for the internal quark and $V_{qq'}$ is the CKM matrix element. After four-momentum integration, the following contribution to the q quark CMDM is obtained:

$$a_q^W(q^2) = \sum_{q'} \frac{G_F m_q^2 |V_{qq'}|^2}{4\sqrt{2}\pi^2} \mathcal{F}_{qq'}^W(q^2), \quad (22)$$

with the dominant term arising from the diagonal CKM matrix element ($V_{qq} \approx 1$). There is no agreement with the result of [26] as those authors consider that the external and internal quark masses are degenerate.

2.2.4 Higgs boson exchange

The remaining SM contribution to the quark CMDM arises from the diagram with Higgs boson exchange. The corresponding contribution to the $\bar{q}qg$ vertex function is given by

$$\Gamma_h^\mu = \frac{ig^2 m_q^2}{4m_W^2} \int \frac{d^D k}{(2\pi)^D} \frac{(q\cancel{k} + m_q) \gamma^\mu (q\cancel{t} + m_q)}{(q_2^2 - m_q^2)(q_1^2 - m_q^2)(k^2 - m_h^2)}. \quad (23)$$

Again, the algebra is straightforward and we obtain after four-momentum integration:

$$a_q^h(q^2) = -\frac{G_F m_q^2}{4\sqrt{2}\pi^2} \mathcal{F}_q^h(q^2), \quad (24)$$

which for $q^2 = 0$ agrees with the results presented in [26].

3 Numerical evaluation and discussion

We now turn to the numerical evaluation of the one-loop contribution to the CMDM of quarks. We first present a numerical estimate of the quark CMDM in the SM, which is aimed to make a comparison with previous results, which can be useful to settle any ambiguity.

3.1 Transition CMDM of quarks in the SM

We first analyze the behavior of the parameter $\hat{\mu}_{-a_q}/2$ in the SM, which is the one studied by the experimental collaborations [21]. Although the top quark CMDM is the one mainly studied in the literature, for the sake of completeness we include in our analysis an estimate for all the SM quarks. Since the results for the QCD contribution have not sense in perturbative calculations at $q^2 = 0$, as pointed out above, we study the case $q^2 \neq 0$. Anomalous top quark couplings have been studied at the LHC through $t\bar{t}$ production [30, 31, 32, 22], where the transition CMDM contributes at the leading order through the diagrams shown in Fig. 3, where we include the $g\bar{g}t\bar{t}$ interaction arising from Lagrangian (1). Since the outgoing top quarks are on-shell, the gluon four-momentum in the s -channel diagrams obeys $\|q\| \geq 2m_t$, whereas in the t and u channels there are no such kinematical constraint.

We have implemented the strong coupling constant $\alpha_s(q^2)$ as the three loop approximate solution of the renormalization group equation of QCD [33, 34]. We consider gluon four-momentum transfer in the 30-1000 GeV region, where $\alpha_s \sim 0.1$, since for $\|q\|$ less than around 1 GeV the theory becomes strongly interacting [35]. In addition, at next-to-leading order QCD calculations, EW corrections are neglected, so only the pure QCD contribution to the CMDM of quarks would be relevant.

For the numerical analysis we use the results in terms of Passarino-Veltman scalar functions, which were evaluated via the LoopTools [36] and Collier [37] packages, though we cross-check with the results obtained by numerical integration of the Feynman parameter results. We also compared our numerical results with those reported in [15]: although there is a good agreement with the real part of the QCD and EW contributions to $\hat{\mu}_t$, we obtain non-zero imaginary parts in the Z , h and QCD₂ contributions, which are absent in previous evaluations.

3.1.1 Light quarks CMDM

We show in Fig. 4 the behavior of the real $\text{Re}[\hat{\mu}_q]$ and imaginary $\text{Im}[\hat{\mu}_q]$ parts of the CMDM of the light SM quarks as functions of the gluon transfer momentum $\|q\|$. We observe that in both cases the largest estimates correspond to the b quark CMDM, whereas the smallest estimates are obtained for the u and d quarks. This stems from the fact that the CMDM is proportional to the quark mass for $q^2 \neq 0$. We also note that the real and imaginary parts of $\hat{\mu}_q$ are about the same magnitude for all the light quarks. Numerical predictions for the CMDM of light quarks are shown in Table 1 for some selected values of $\|q\|$.

We now turn to analyze the behavior of the partial contributions to $\hat{\mu}_q$ for a light quark. Thus, by way of illustration, we show in Fig. 5 the real and imaginary parts of the partial contributions to the c quark CMDM. All other light quark's contributions exhibit a similar behavior, though there are slight changes for the b quark as explained below. We first note that the dominant contributions arise from the triple gluon vertex (the so-called QCD₂ contribution), though at high energies the QCD₁, γ , Z and W contributions are of similar size. In particular, the imaginary parts of the EW gauge bosons contributions are slightly larger than the one of the QCD₁ contribution for $\|q\| \gtrsim 600$ GeV, whereas the real parts of both QCD contributions dominate in all the studied energy interval. On the other hand, the Higgs boson contributions are the smallest ones: for the u and d quarks, such contributions are

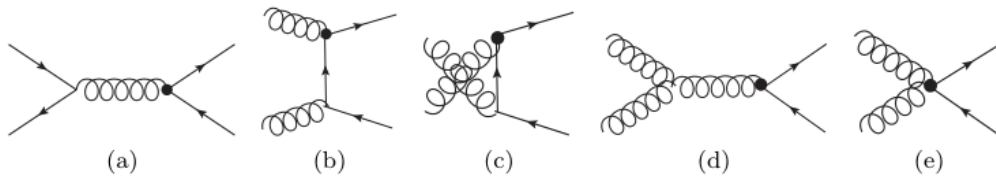


Fig. 3 Feynman diagrams for tt production via the Lagrangian of Fig. 1.

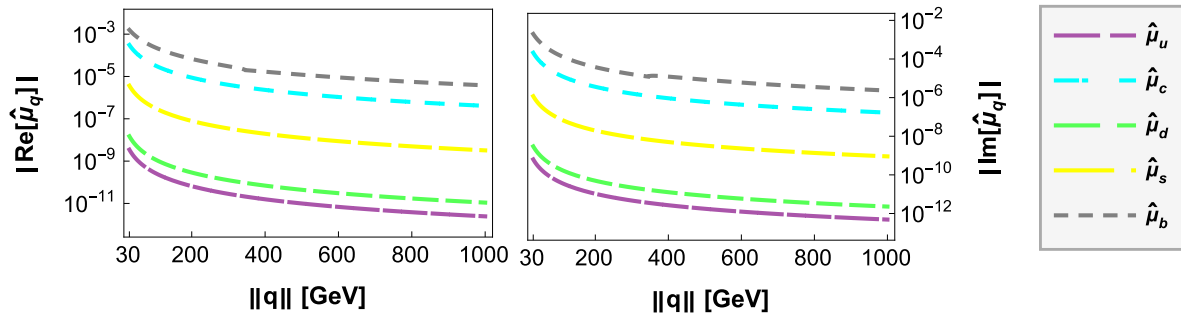


Fig. 4 Real (left plot) and imaginary (right plot) parts of the light quarks CMDM $\hat{\mu}_q$ as function of the transfer momentum of the gluon.

negligibly small, of the order of $10^{-20} - 10^{-21}$. Note that for $\|q\| > 30$ GeV all the partial contributions to $\hat{\mu}_q$ develop an imaginary part as $q^2 > 4m^2$, with m the mass of the virtual particles attached to the external gluon, except for the W contribution to $\hat{\mu}_b$, which is purely real for $q^2 < 4m_t^2$ as long as one neglects the contributions of the loops with internal u and c quarks.

3.1.2 Top quark CMDM

We now turn to analyze the behavior of the CMDM of the top quark. We first show in Fig. 6 $\hat{\mu}_t$ as a function of $\|q\|$ as well as its partial QCD and EW contributions. We observe that both the real and imaginary parts are dominated by the QCD contributions, though the real part of the EW contribution is of comparable size around the threshold $\|q\| = 2m_t$, where all the contributions show a peak due to a flip of sign. Both the QCD and EW contributions decrease as $\|q\|$ increases: above the $2m_t$ threshold the real part of the EW contribution becomes negligible, whereas its imaginary part is about one order of magnitude below the imaginary part of the QCD contribution for $\|q\| \sim 1000$ GeV. However, at very large $\|q\|$ (much larger than 1000 GeV) the imaginary part of the EW contribution becomes dominant since the imaginary part of the QCD contribution decreases quickly at very high energies.

We now show in Fig. 7 the real and imaginary parts of all the partial contributions to $\hat{\mu}_t$ as functions of $\|q\|$. As far as the real parts are concerned, we observe

that at low and high energies the QCD_2 contribution dominates, but around $\|q\| = 2m_t$ the Z and h contributions become the dominant ones, which explains the behavior of the EW contribution shown in Fig. 6 at $\|q\| \simeq 2m_t$. Nevertheless such contributions are of opposite sign and they tend to cancel each other out. On the other hand, as for the imaginary contributions, below the threshold $\|q\| = 2m_t$ all but the QCD_2 and W contributions vanish and above this threshold the Z and h contributions develop imaginary parts of the same order of magnitude than that of the three-gluon contribution (QCD_2), which remains slightly larger as $\|q\|$ increases. We can conclude that the QCD contributions is always dominant, nevertheless the imaginary part of the EW contribution become comparable to the QCD one at high energies. After the threshold $\|q\| = 2m_t$ the top quark CMDM exhibits a peak due to a flip of sign. Such a behavior is not observed however in the CEDM of light quarks as we are studying energies far from the threshold region.

Finally, we show in Table 1 the numerical estimates of $\hat{\mu}_q$ for all the SM quarks at a few selected values of the gluon transfer momentum $\|q\|$. As expected, the largest estimate corresponds the top quark CMDM, though the bottom and charm quarks CMDM could also be non-negligible in some energy regions. The CMDM of all quarks is in general complex, with real and imaginary parts of comparable size, though the real parts are always slightly larger.

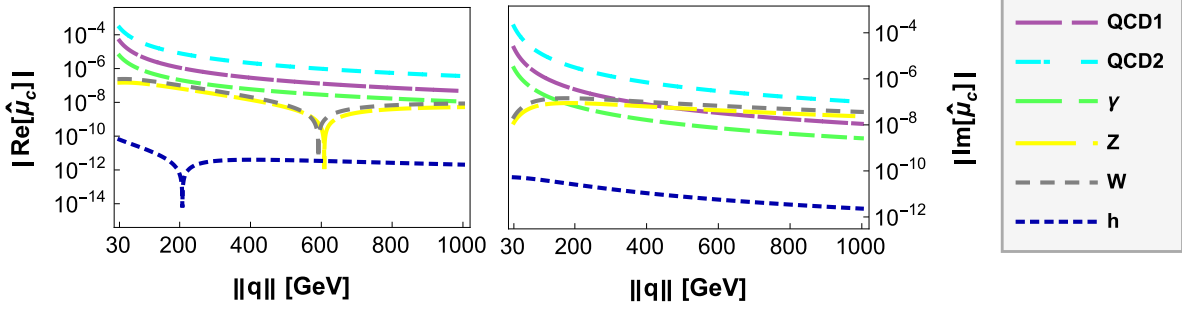


Fig. 5 Real (left plot) and imaginary (right plot) parts of the SM one-loop partial contributions to $\hat{\mu}_c$ as functions of the transfer momentum of the gluon $\|q\|$.

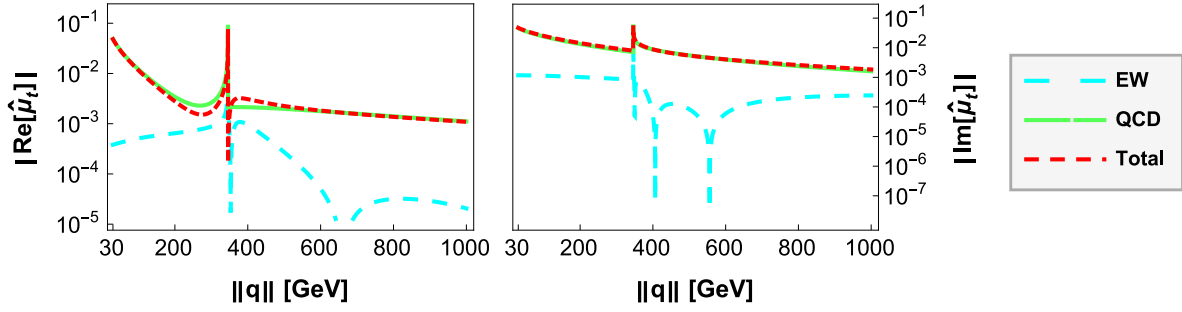


Fig. 6 Real (left plot) and imaginary (right plot) parts of the EW, QCD and total contributions to the top quark CDMM $\hat{\mu}_t$ as function of the transfer momentum norm of the gluon $\|q\|$.

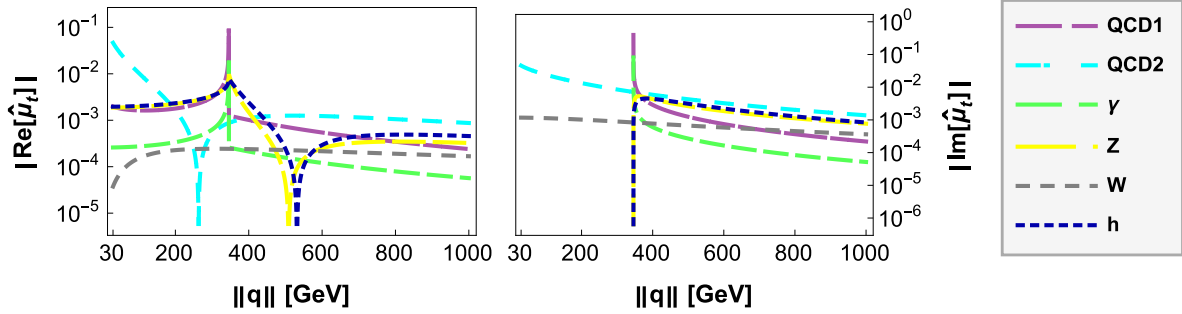


Fig. 7 Real (left plot) and imaginary (right plot) parts of the SM one-loop partial contributions to the top quark CDMM $\hat{\mu}_t$ as functions of the transfer momentum of the gluon $\|q\|$.

Table 1 Estimates for the SM contribution to the CDMM $\hat{\mu}_q$ of the SM quarks for select values of the gluon transfer momentum $\|q\|$.

Quark	$\ q\ = 30 \text{ GeV}$	$\ q\ = m_Z$	$\ q\ = 500 \text{ GeV}$
d	$1.47 \times 10^{-8} - i2.96 \times 10^{-9}$	$1.44 \times 10^{-9} - i2.55 \times 10^{-10}$	$4.33 \times 10^{-11} - i8.21 \times 10^{-12}$
u	$3.47 \times 10^{-9} - i6.33 \times 10^{-10}$	$3.35 \times 10^{-10} - i5.47 \times 10^{-11}$	$9.94 \times 10^{-12} - i1.75 \times 10^{-12}$
s	$3.63 \times 10^{-6} - i1.17 \times 10^{-6}$	$3.8 \times 10^{-7} - i1.01 \times 10^{-7}$	$1.23 \times 10^{-8} - i3.25 \times 10^{-9}$
c	$3.08 \times 10^{-4} - i2.10 \times 10^{-4}$	$3.96 \times 10^{-5} - i1.87 \times 10^{-5}$	$1.51 \times 10^{-6} - i6.07 \times 10^{-7}$
b	$1.55 \times 10^{-3} - i1.95 \times 10^{-3}$	$2.72 \times 10^{-4} - i1.96 \times 10^{-4}$	$1.24 \times 10^{-5} - i6.56 \times 10^{-6}$
t	$-4.81 \times 10^{-2} - i4.69 \times 10^{-2}$	$-1.33 \times 10^{-2} - i2.66 \times 10^{-2}$	$2.24 \times 10^{-3} - i5.43 \times 10^{-3}$

4 Conclusions

In this work we present a new evaluation of the SM prediction of the CMDM $\hat{\mu}_q$ of quarks at the one-loop level, which is aimed to address some inconsistencies appearing in previous calculations. We considered the most general case with non-zero transfer momentum of the gluon q^2 and present results for the corresponding loop integrals in terms of Feynman parameter integrals, emphasizing the disagreements with previous evaluations. For completeness our results are also presented in terms of Passarino-Veltman scalar functions and closed form functions, which have never been presented in the literature to our knowledge and may serve as a cross-check for the numerical calculation. It is found that the QCD contribution arising from the Feynman diagram with a three-gluon vertex is not well defined at $q^2 = 0$, which is due to the fact that the static CMDM has not perturbative sense, as it has been also pointed out by the authors of Refs. [26, 15]. We then perform a numerical analysis and examine the behavior of the CMDM of all the SM quarks in the region $30 \text{ GeV} < \|q\| < 1000 \text{ GeV}$, where the QCD coupling constant $\alpha(q^2)$ is of the order of 10^{-1} . In this energy region the CMDM are complex in general, with the imaginary parts being about the same order of magnitude than the real parts. Furthermore, the QCD contributions dominate over the EW contributions, which suggests that two-loop contributions can be relevant. On the other hand, the imaginary part of the EW contribution is only comparable to the QCD contribution at very high energies. Since the CMDM is proportional to the quark mass, the largest contributions correspond to the top quark CMDM, which is of the order of $10^{-2} - 10^{-3}$, with the imaginary part of the EW contributions of the same size than the QCD contributions around the threshold $q^2 = 4m_t^2$.

Note Added: After this work was submitted, we became aware that a very related paper [38], that focuses on the top quark CMDM only, had been recently posted to the preprint archive. Our conclusions and numerical estimates for the top quark CMDM agree with those presented in that paper, which only considers the case with $q^2 = \mp m_Z^2$.

Acknowledgements We acknowledge support from Consejo Nacional de Ciencia y Tecnología and Sistema Nacional de Investigadores. Partial support from Vicerrectoría de Investigación y Estudios de Posgrado de la Benémerita Universidad Autónoma de Puebla is also acknowledged.

Appendix A: Analytic results for the loop functions

We now present the results for the loop functions appearing in the contributions to the CMDM of quarks discussed in Sec. 2 in term of Feynman parameter integrals, Passarino-Veltman scalar functions, and closed form functions. For sake of completeness we also include the results for $q^2 = 0$.

Appendix A.1: Feynman parameter integrals

We introduce the definition $r_{a,b} = m_a/m_b$ and present the loop functions for the QCD contributions to the CMDM of quarks. Feynman diagram 2(a) yields the loop function [Eq. (7)]:

$$\mathcal{F}_q^{\text{QCD}_1}(q^2) = m_q^2 \int_0^1 \int_0^{1-u} \frac{(u-1)u}{m_q^2(u-1)^2 + q^2v(u+v-1)} dvdu, \quad (\text{A.1})$$

whereas Feynman diagram 2(b) gives [Eq. (12)]:

$$\mathcal{F}_q^{\text{QCD}_2}(q^2) = m_q^2 \int_0^1 \int_0^{1-u} \frac{(u-1)u}{m_q^2u^2 - q^2v(1-u-v)} dvdu, \quad (\text{A.2})$$

which for $q^2 = 0$ reduces to

$$\mathcal{F}_q^{\text{QCD}_2}(0) = \int_0^1 \frac{(1-u)^2}{u} du. \quad (\text{A.3})$$

As far as the EW contributions to the CMDM of quarks are concerned, the Feynman diagram with photon exchange of Fig. 1(a) gives [Eq. (15)]:

$$\mathcal{F}_q^A(q^2) = m_q^2 \int_0^1 \int_0^{1-u} \frac{(u-1)u}{m_q^2(u-1)^2 + q^2v(u+v-1)} dvdu, \quad (\text{A.4})$$

whereas the Z boson exchange diagram gives [Eq. (19)]

$$\mathcal{A}_q^Z(q^2) = \int_0^1 \int_0^{1-u} \frac{dudv}{\Delta_Z} \left((3u-1)\Delta_Z \log\left(\frac{\Delta_Z}{\mu^2}\right) + 2(m_q^2(u-1)^3 - 2m_Z^2u) + 2q^2uv(u+v-1) \right), \quad (\text{A.5})$$

and

$$\mathcal{V}_q^Z(q^2) = - \int_0^1 \int_0^{1-u} \frac{dudv}{\Delta_Z} m_Z^2(u-1)u, \quad (\text{A.6})$$

where $\Delta_Z = m_q^2(u-1)^2 + m_Z^2u + q^2v(u+v-1)$ and μ is the scale of dimensional regularization, which cancels out after integration.

For $q^2 = 0$, the last two loop functions give:

$$\mathcal{A}_q^Z(0) = \int_0^1 du \frac{u(2u^2 + r_{Z,q}^2(u-4)(u-1))}{r_{Z,q}^2(u-1) - u^2}, \quad (\text{A.7})$$

and

$$\mathcal{V}_q^Z(0) = \int_0^1 du \frac{g_V^q r_{Z,q}^2(u-1)u^2}{r_{Z,q}^2(u-1) - u^2}. \quad (\text{A.8})$$

As for the W boson exchange contribution of diagram 1(b), it is given by [Eq. (22)]:

$$\mathcal{F}_{qq'}^W(q^2) = \int_0^1 \int_0^{1-u} \frac{dudv}{\Delta_W} \left(- (1-3u) \log\left(\frac{\Delta_W}{\mu^2}\right) \Delta_W - 2m_{q'}^2(u-1)^2 + u(2m_q^2(u-1)^2 - m_W^2(u+3) + 2q^2v(u+y-1)) \right), \quad (\text{A.9})$$

with the following result for $q^2 = 0$:

$$\mathcal{F}_{qq'}^W(0) = \int_0^1 \frac{u \left[u \left((u-1) + r_{q',q}^2 (u+1) \right) + 2r_{W,q}^2 (u-2)(u-1) \right]}{r_{W,q}^2 (u-1) - u \left((u-1) + r_{q',q}^2 \right)} du, \quad (\text{A.10})$$

where $\Delta_W = u (m_q^2 (u-1) + m_W^2) - m_{q'}^2 (u-1) + q^2 v (u+v-1)$.

Finally, for the Higgs contribution [Eq. (24)] we obtain:

$$\mathcal{F}_q^h(q^2) = m_q^2 \int_0^1 \int_0^{1-u} \frac{(u^2-1)}{m_q^2 (u-1)^2 + u m_h^2 + q^2 v (u+v-1)} dv du, \quad (\text{A.11})$$

which for $q^2 = 0$ reduces to

$$\mathcal{F}_q^h(0) = - \int_0^1 du \frac{(1+u)(1-u)^2}{(1-u)^2 + u r_{h,q}^2}. \quad (\text{A.12})$$

Appendix A.2: Passarino-Veltman results

We now present the above results in terms of Passarino-Veltman scalar integrals, where we use the standard notation for the two- and three-point scalar functions. Also we define $\xi(x, y) = \sqrt{x^2 - 4y^2}$. The loop functions are

$$\mathcal{F}_q^{\text{QCD}_1}(q^2) = \frac{m_q^2}{\xi^2(\|q\|, m_q)} \left\{ \mathbf{B}_0(0; m_q, m_q) - \mathbf{B}_0(q^2; m_q, m_q) + 2 \right\}, \quad (\text{A.13})$$

$$\begin{aligned} \mathcal{F}_q^{\text{QCD}_2}(q^2) &= \frac{m_q^2}{\xi^4(\|q\|, m_q)} \left\{ (8m_q^2 + q^2) (\mathbf{B}_0(0; m_q, m_q) - \mathbf{B}_0(q^2; 0, 0)) \right. \\ &\quad \left. - 6m_q^2 (q^2 \mathbf{C}_0(m_q^2, m_q^2, q^2; 0, m_q, 0) - 4) \right\}, \end{aligned} \quad (\text{A.14})$$

$$\mathcal{F}_q^{\text{QCD}_2}(0) = \frac{1}{2} \left\{ \mathbf{B}_0(0; m_q, m_q) + 3 \right\}, \quad (\text{A.15})$$

$$\mathcal{F}_q^A(q^2) = \frac{m_q^2}{\xi^2(\|q\|, m_q)} \left\{ \mathbf{B}_0(0; m_q, m_q) - \mathbf{B}_0(q^2; m_q, m_q) + 2 \right\}, \quad (\text{A.16})$$

$$\begin{aligned} \mathcal{A}_q^Z(q^2) &= \frac{m_Z^2}{m_q^2 \xi^4(\|q\|, m_q)} \left\{ \left(q^2 (m_Z^2 - 8m_q^2) + 10m_q^2 (2m_q^2 - m_Z^2) \right) \mathbf{B}_0(m_q^2; m_q, m_Z) \right. \\ &\quad + \frac{m_q^2}{m_Z^2} \left(q^2 (9m_Z^2 - 2m_q^2) + (8m_q^4 - 24m_q^2 m_Z^2 + 6m_Z^4) \right) \mathbf{B}_0(q^2; m_q, m_q) \\ &\quad + \frac{(2m_q^2 + m_Z^2) \xi^2(\|q\|, m_q)}{m_Z^2} \left(m_q^2 \mathbf{B}_0(0; m_q, m_q) - m_Z^2 \mathbf{B}_0(0; m_Z, m_Z) \right) \\ &\quad + 2 \left(2q^2 (3m_Z^2 - 7m_q^2) + 2q^4 + 3 (8m_q^4 - 6m_q^2 m_Z^2 + m_Z^4) \right) m_q^2 \mathbf{C}_0(m_q^2, m_q^2, q^2; m_q, m_Z, m_q) \\ &\quad \left. + \frac{(4m_q^4 - m_Z^4) \xi^2(\|q\|, m_q)}{m_Z^2} \right\}, \end{aligned} \quad (\text{A.17})$$

$$\begin{aligned}
\mathcal{V}_q^Z(q^2) &= \frac{m_Z^2}{m_q^2 \xi^4(\|q\|, m_q)} \left\{ \left(q^2 (m_Z^2 - 2m_q^2) + 2m_q^2 (4m_q^2 - 5m_Z^2) \right) \mathbf{B}_0(m_q^2; m_q, m_Z) \right. \\
&\quad + m_q^2 \left(2(3m_Z^2 - 2m_q^2) + q^2 \right) \mathbf{B}_0(q^2; m_q, m_q) + \xi^2(\|q\|, m_q) \left(m_q^2 \mathbf{B}_0(0; m_q, m_q) - m_Z^2 \mathbf{B}_0(0; m_Z, m_Z) \right) \\
&\quad \left. + \left(4q^2 + 2(3m_Z^2 - 8m_q^2) \right) m_q^2 m_Z^2 \mathbf{C}_0(m_q^2, m_q^2, q^2; m_q, m_Z, m_q) + (2m_q^2 - m_Z^2) \xi^2(\|q\|, m_q) \right\}, \tag{A.18}
\end{aligned}$$

$$\begin{aligned}
\mathcal{A}_q^Z(0) &= \frac{m_Z^2}{8m_q^4} \left\{ \left(10m_q^2 - 5m_Z^2 \right) \mathbf{B}_0(m_q^2; m_q, m_Z) + \left(3m_Z^2 - 14m_q^2 \right) \mathbf{B}_0(0; m_q, m_q) \right. \\
&\quad + 2 \left(2m_q^2 + m_Z^2 \right) \mathbf{B}_0(0; m_Z, m_Z) + 3 \left(m_Z^4 - 6m_q^2 m_Z^2 + 8m_q^4 \right) \mathbf{C}_0(m_q^2, m_q^2, 0; m_q, m_Z, m_q) \\
&\quad \left. + \frac{2}{m_Z^2} \left(m_Z^4 - 4m_q^4 \right) \right\}, \tag{A.19}
\end{aligned}$$

$$\begin{aligned}
\mathcal{V}_q^Z(0) &= \frac{m_Z^2}{8m_q^4} \left\{ \left(4m_q^2 - 5m_Z^2 \right) \mathbf{B}_0(m_q^2; m_q, m_Z) + \left(3m_Z^2 - 4m_q^2 \right) \mathbf{B}_0(0; m_q, m_q) \right. \\
&\quad \left. + 2m_Z^2 \mathbf{B}_0(0; m_Z, m_Z) + \left(3m_Z^2 - 8m_q^2 \right) m_Z^2 \mathbf{C}_0(m_q^2, m_q^2, 0; m_q, m_Z, m_q) + 2 \left(m_Z^2 - 2m_q^2 \right) \right\}, \tag{A.20}
\end{aligned}$$

$$\begin{aligned}
\mathcal{F}_{qq'}^W(q^2) &= \frac{1}{m_q^2 \xi^4(\|q\|, m_q)} \left\{ \xi^2(\|q\|, m_q) \left(m_q^2 + m_{q'}^2 + 2m_W^2 \right) \left(m_{q'}^2 \mathbf{B}_0(0; m_{q'}, m_{q'}) - m_W^2 \mathbf{B}_0(0; m_W, m_W) \right) \right. \\
&\quad - \left[q^2 \left(m_q^4 + m_q^2 \left(9m_W^2 - 2m_{q'}^2 \right) + m_{q'}^4 + m_{q'}^2 m_W^2 - 2m_W^4 \right) + 2m_q^2 \left(m_q^4 + m_q^2 \left(4m_{q'}^2 - 9m_W^2 \right) \right. \right. \\
&\quad \left. \left. - 5 \left(m_{q'}^4 + m_{q'}^2 m_W^2 - 2m_W^4 \right) \right) \right] \mathbf{B}_0(m_q^2; m_{q'}, m_W) + m_q^2 \left[q^2 \left(m_q^2 - 3m_{q'}^2 + 10m_W^2 \right) \right. \\
&\quad \left. + 2 \left(m_q^4 + m_q^2 \left(6m_{q'}^2 - 11m_W^2 \right) - 3 \left(m_{q'}^4 + m_{q'}^2 m_W^2 - 2m_W^4 \right) \right) \right] \mathbf{B}_0(q^2; m_{q'}, m_{q'}) \\
&\quad - 2m_q^2 \left[m_q^2 \left(m_q^4 - m_q^2 \left(5m_{q'}^2 + 12m_W^2 \right) + \left(7m_{q'}^4 - 12m_{q'}^2 m_W^2 + 17m_W^4 \right) \right) - 3 \left(m_{q'}^6 - 3m_{q'}^2 m_W^4 + 2m_W^6 \right) \right. \\
&\quad \left. - q^2 \left(m_q^4 - 2m_q^2 \left(m_{q'}^2 + 4m_W^2 \right) + m_{q'}^4 - 6m_{q'}^2 m_W^2 + 8m_W^4 \right) - 2m_W^2 \left(q^2 \right)^2 \right] \mathbf{C}_0(m_q^2, m_q^2, q^2; m_{q'}, m_W, m_{q'}) \\
&\quad \left. + \xi^2(\|q\|, m_q) \left(m_q^2 + m_{q'}^2 - m_W^2 \right) \left(m_q^2 + m_{q'}^2 + 2m_W^2 \right) \right\}, \tag{A.21}
\end{aligned}$$

$$\begin{aligned}
\mathcal{F}_{qq'}^W(0) &= \frac{1}{8m_q^4} \left\{ 2m_W^2 \left(m_q^2 + m_{q'}^2 + 2m_W^2 \right) \mathbf{B}_0(0; m_W, m_W) + \left[m_q^4 + m_q^2 \left(4m_{q'}^2 - 11m_W^2 \right) \right. \right. \\
&\quad \left. \left. - 5m_{q'}^4 - 7m_{q'}^2 m_W^2 + 6m_W^4 \right] \mathbf{B}_0(0; m_{q'}, m_{q'}) - \left[m_q^4 + m_q^2 \left(4m_{q'}^2 - 9m_W^2 \right) \right. \right. \\
&\quad \left. \left. - 5 \left(m_{q'}^4 + m_{q'}^2 m_W^2 - 2m_W^4 \right) \right] \mathbf{B}_0(m_q^2; m_{q'}, m_W) + \left[12m_q^2 m_W^2 \left(m_q^2 + m_{q'}^2 \right) \right. \right. \\
&\quad \left. \left. - m_W^4 \left(17m_q^2 + 9m_{q'}^2 \right) - \left(m_q^2 - 3m_{q'}^2 \right) \left(m_q^2 - m_{q'}^2 \right)^2 + 6m_W^6 \right] \mathbf{C}_0(m_q^2, m_q^2, 0; m_{q'}, m_W, m_{q'}) \right. \\
&\quad \left. - 2 \left(m_q^2 + m_{q'}^2 - m_W^2 \right) \left(m_q^2 + m_{q'}^2 + 2m_W^2 \right) \right\}, \tag{A.22}
\end{aligned}$$

$$\begin{aligned}
\mathcal{F}_q^h(q^2) &= \frac{1}{\xi^4(\|q\|, m_q)} \left\{ \xi^2(\|q\|, m_q) \left(m_h^2 \mathbf{B}_0(0; m_h, m_h) - m_q^2 \mathbf{B}_0(0; m_q, m_q) \right) \right. \\
&\quad + \left(4m_q^2 \xi^2(\|q\|, m_q) + m_h^2 (10m_q^2 - q^2) \right) \mathbf{B}_0(m_q^2; m_q, m_h) - 3m_q^2 \left(\xi^2(\|q\|, m_q) - 2m_h^2 \right) \mathbf{B}_0(q^2; m_q, m_q) \\
&\quad \left. - 6m_h^2 m_q^2 \left(\xi^2(\|q\|, m_q) + m_h^2 \right) \mathbf{C}_0(m_q^2, m_q^2, q^2; m_q, m_h, m_q) + \left(m_h^2 - 2m_q^2 \right) \xi^2(\|q\|, m_q) \right\}, \tag{A.23}
\end{aligned}$$

and

$$\begin{aligned} \mathcal{F}_q^h(0) = & -\frac{1}{8m_q^2} \left\{ (3m_h^2 - 8m_q^2) \mathbf{B}_0(0; m_q, m_q) + (8m_q^2 - 5m_h^2) \mathbf{B}_0(m_q^2; m_q, m_h) \right. \\ & + 2m_h^2 \mathbf{B}_0(0; m_h, m_h) + 3m_h^2 (m_h^2 - 4m_q^2) \mathbf{C}_0(m_q^2, m_q^2, 0; m_q, m_h, m_q) \\ & \left. + 2(m_h^2 - 2m_q^2) \right\}. \end{aligned} \quad (\text{A.24})$$

Appendix A.3: Closed form results

We also present the explicit solutions for the two-point scalar functions in terms of closed form functions. Below $C_0(m_i^2, m_j^2, q^2; m_k, m_l, m_n)$ stands for a three-point Passarino-Veltman scalar function.

$$\mathcal{F}_q^{\text{QCD}_1}(q^2) = -\frac{m_q^2}{\|q\|\xi(\|q\|, m_q)} \log \left(\frac{\|q\|\xi(\|q\|, m_q) + 2m_q^2 - q^2}{2m_q^2} \right), \quad (\text{A.25})$$

$$\begin{aligned} \mathcal{F}_q^{\text{QCD}_2}(q^2) = & -\frac{m_q^2}{\xi^4(\|q\|, m_q)} \left\{ q^2 \left[6m_q^2 C_0(m_q^2, m_q^2, q^2; 0, m_q, 0) + \log \left(\frac{m_q^2}{q^2} \right) + 2 + i\pi \right] \right. \\ & \left. + 8m_q^2 \left[\log \left(\frac{m_q^2}{q^2} \right) - 1 + i\pi \right] \right\}, \end{aligned} \quad (\text{A.26})$$

$$\mathcal{F}_q^{\text{QCD}_2}(0) = \frac{1}{2} \left\{ \frac{1}{\epsilon} + \log \left(\frac{\mu^2}{m_q^2} \right) + 3 \right\}, \quad (\text{A.27})$$

$$\mathcal{F}_q^A(q^2) = -\frac{m_q^2}{\|q\|\xi(\|q\|, m_q)} \log \left(\frac{\|q\|\xi(\|q\|, m_q) + 2m_q^2 - q^2}{2m_q^2} \right), \quad (\text{A.28})$$

$$\begin{aligned} \mathcal{A}_q^Z(q^2) = & \frac{m_Z^2}{2m_q^2 \xi^4(\|q\|, m_q)} \left\{ \left(20m_Z (2m_q^2 - m_Z^2) + \frac{2m_Z (m_Z^2 - 8m_q^2) q^2}{m_q^2} \right) \xi(m_Z, m_q) \log \left(\frac{m_Z + \xi(m_Z, m_q)}{2m_q} \right) \right. \\ & + 2 \left(\frac{(9m_Z^2 - 2m_q^2)}{m_Z^2} + \frac{(8m_q^4 - 24m_Z^2 m_q^2 + 6m_Z^4)}{m_Z^2 q^2} \right) m_q^2 \|q\| \xi(\|q\|, m_q) \log \left(\frac{2m_q^2 - q^2 + \|q\|\xi(\|q\|, m_q)}{2m_q^2} \right) \\ & + \left(2(8m_q^4 + 14m_Z^2 m_q^2 - 5m_Z^4) + \frac{(-4m_q^4 - 10m_Z^2 m_q^2 + m_Z^4) q^2}{m_q^2} \right) \log \left(\frac{m_q^2}{m_Z^2} \right) \\ & + \left(8(q^2)^2 + 12(8m_q^4 - 6m_Z^2 m_q^2 + m_Z^4) + 8(3m_Z^2 - 7m_q^2) q^2 \right) m_q^2 C_0(m_q^2, m_q^2, q^2; m_q, m_Z, m_q) \\ & \left. + 2(2m_q^2 + m_Z^2) \xi^2(\|q\|, m_q) \right\}, \end{aligned} \quad (\text{A.29})$$

$$\begin{aligned} \mathcal{V}_q^Z(q^2) = & \frac{m_Z^2}{2m_q^2 \xi^4(\|q\|, m_q)} \left\{ 2m_Z^2 \left((3m_Z^2 - 8m_q^2) + 2q^2 \right) m_q^2 C_0(m_q^2, m_q^2, q^2; m_q, m_Z, m_q) \right. \\ & + \left(\frac{4(3m_Z^2 - 2m_q^2)}{q^2} + 2 \right) m_q^2 \|q\| \xi^2(\|q\|, m_q) \log \left(\frac{2m_q^2 - q^2 + \|q\|\xi(\|q\|, m_q)}{2m_q^2} \right) \\ & + 2m_Z^2 \xi(\|q\|, m_q) + \left(2m_Z^2 (8m_q^2 - 5m_Z^2) + \frac{m_Z^2 \xi^2(m_Z, m_q) q^2}{m_q^2} \right) \log \left(\frac{m_q^2}{m_Z^2} \right) \\ & \left. + \left(4m_Z (4m_q^2 - 5m_Z^2) + \frac{2m_Z (m_Z^2 - 2m_q^2) q^2}{m_q^2} \right) \xi(m_Z, m_q) \log \left(\frac{m_Z + \xi(m_Z, m_q)}{2m_q} \right) \right\}, \end{aligned} \quad (\text{A.30})$$

$$\begin{aligned} \mathcal{A}_q^Z(0) = & \frac{m_Z^2}{2m_q^6} \left\{ -\frac{m_q^2(m_q^2 - 2m_Z^2)(2m_q^2 - m_Z^2)}{m_Z^2} + (-2m_q^4 + 4m_q^2 m_Z^2 - m_Z^4) \log\left(\frac{m_q^2}{m_Z^2}\right) \right. \\ & \left. - \frac{2(8m_q^4 - 6m_q^2 m_Z^2 + m_Z^4)m_Z}{\xi(m_Z, m_q)} \log\left(\frac{m_Z + \xi(m_Z, m_q)}{2m_q}\right) \right\}, \end{aligned} \quad (\text{A.31})$$

$$\begin{aligned} \mathcal{V}_q^Z(0) = & \frac{m_Z^2}{2m_q^6} \left\{ m_q^2(m_q^2 - 2m_Z^2) - m_Z^2(m_Z^2 - 2m_q^2) \log\left(\frac{m_q^2}{m_Z^2}\right) \right. \\ & \left. - \frac{2(2m_q^4 - 4m_q^2 m_Z^2 + m_Z^4)}{\xi(m_Z, m_q)} \log\left(\frac{\xi(m_Z, m_q) + m_Z}{2m_q}\right) \right\}, \end{aligned} \quad (\text{A.32})$$

$$\begin{aligned} \mathcal{F}_{qq'}^W(q^2) = & \frac{1}{2m_q^2 \xi^4(\|q\|, m_q)} \left\{ -4m_q^2(m_q^6 - m_q^4(5m_{q'}^2 + 12m_W^2) + m_q^2(7m_{q'}^4 - 12m_{q'}^2 m_W^2 + 17m_W^4)) \right. \\ & - q^2(m_q^4 - 2m_q^2(m_{q'}^2 + 4m_W^2) + m_{q'}^4 - 6m_{q'}^2 m_W^2 + 8m_W^4) - 3(m_{q'}^6 - 3m_{q'}^2 m_W^4 + 2m_W^6) \\ & - 2m_W^2(q^2)^2 C_0(m_q^2, m_q^2, q^2; m_{q'}, m_W, m_{q'}) + 2\xi^2(\|q\|, m_q)(m_q^4 + 3m_q^2 m_W^2 - m_{q'}^4 - m_{q'}^2 m_W^2 + 2m_W^4) \\ & + \frac{2m_q^2}{q^2} \|q\| \xi(\|q\|, m_{q}') (2(m_q^4 + m_q^2(6m_{q'}^2 - 11m_W^2) - 3(m_{q'}^4 + m_{q'}^2 m_W^2 - 2m_W^4))) \\ & + q^2(-3m_{q'}^2 + m_q^2 + 10m_W^2) \log\left(\frac{\|q\| \xi(\|q\|, m_{q}') + 2m_{q'}^2 - q^2}{2m_{q'}^2}\right) \\ & - \frac{2}{m_q^2} \sqrt{((m_q - m_{q}')^2 - m_W^2)((m_q + m_{q}')^2 - m_W^2)} (q^2(m_q^4 + m_q^2(9m_W^2 - 2m_{q'}^2) + m_{q'}^4 + m_{q'}^2 m_W^2 \\ & - 2m_W^4) + 2m_q^2(m_q^4 + m_q^2(4m_{q'}^2 - 9m_W^2) - 5(m_{q'}^4 + m_{q'}^2 m_W^2 - 2m_W^4))) \\ & \times \log\left(\frac{\sqrt{((m_q - m_{q}')^2 - m_W^2)((m_q + m_{q}')^2 - m_W^2)} + m_{q'}^2 - m_q^2 + m_W^2}{2m_{q'} m_W}\right) \\ & - \frac{1}{m_q^2} (q^2(m_q^6 - 3m_q^4(m_{q'}^2 - 4m_W^2) + m_q^2(3m_{q'}^4 - 8m_{q'}^2 m_W^2 + 11m_W^4)) \\ & - m_{q'}^6 + 3m_{q'}^2 m_W^4 - 2m_W^6) + 2m_q^2(m_q^6 + 3m_q^4(m_{q'}^2 - 4m_W^2) + m_q^2(-9m_{q'}^4 + 4m_{q'}^2 m_W^2 - 7m_W^4) \\ & + 5(m_{q'}^6 - 3m_{q'}^2 m_W^4 + 2m_W^6))) \log\left(\frac{m_{q'}^2}{m_W^2}\right) \left. \right\}, \end{aligned} \quad (\text{A.33})$$

$$\begin{aligned} \mathcal{F}_{qq'}^W(0) = & \frac{1}{2m_q^6} \left\{ m_q^2(-m_q^4 - m_q^2(3m_{q'}^2 - 4m_W^2) + 2(m_{q'}^4 + m_{q'}^2 m_W^2 - 2m_W^4)) \right. \\ & - (m_q^4 m_{q'}^2 + m_q^2(-2m_{q'}^4 + 2m_{q'}^2 m_W^2 - 3m_W^4) + m_{q'}^6 - 3m_{q'}^2 m_W^4 + 2m_W^6) \log\left(\frac{m_{q'}^2}{m_W^2}\right) \\ & - \frac{2}{\sqrt{((m_q - m_{q}')^2 - m_W^2)((m_q + m_{q}')^2 - m_W^2)}} (m_q^6 m_{q'}^2 + m_q^4(-3m_{q'}^4 + m_{q'}^2 m_W^2 + 3m_W^4) \\ & + m_q^2(3m_{q'}^6 - 2m_{q'}^4 m_W^2 + 4m_{q'}^2 m_W^4 - 5m_W^6) - (m_{q'}^2 - m_W^2)^3(m_{q'}^2 + 2m_W^2)) \\ & \times \log\left(\frac{\sqrt{((m_q - m_{q}')^2 - m_W^2)((m_q + m_{q}')^2 - m_W^2)} + m_{q'}^2 - m_q^2 + m_W^2}{2m_{q'} m_W}\right) \left. \right\}, \end{aligned} \quad (\text{A.34})$$

$$\begin{aligned}
\mathcal{F}_q^h(q^2) = & -\frac{1}{2m_q^2\xi^4(\|q\|, m_q)} \left\{ 12m_q^4m_h^2 (\xi(\|q\|, m_q) + m_h^2) C_0(m_q^2, m_q^2, q^2; m_q, m_h, m_q) \right. \\
& + 2m_q^2m_h^2\xi(\|q\|, m_q) + \frac{6m_q^4}{q^2}\|q\|\xi(\|q\|, m_q) (\xi^2(\|q\|, m_q) + 2m_h^2) \log\left(\frac{\|q\|\xi(\|q\|, m_q) + 2m_q^2 - q^2}{2m_q^2}\right) \\
& + m_h^2(24m_q^4 + q^2(m_h^2 - 6m_q^2) - 10m_q^2m_h^2) \log\left(\frac{m_q^2}{m_h^2}\right) \\
& \left. - 2m_h\xi(m_h, m_q) (-16m_q^4 - q^2\xi(m_h, m_q) + 10m_q^2m_h^2) \log\left(\frac{\xi(m_h, m_q) + m_h}{2m_q}\right) \right\}, \tag{A.35}
\end{aligned}$$

and

$$\begin{aligned}
\mathcal{F}_q^h(0) = & -\frac{1}{2m_q^4} \left\{ m_q^2(3m_q^2 - 2m_h^2) + 2m_h(m_q^2 - m_h^2) \xi(m_h, m_q) \log\left(\frac{\xi(m_h, m_q) + m_h}{2m_q}\right) \right. \\
& \left. + m_h^2(3m_q^2 - m_h^2) \log\left(\frac{m_q^2}{m_h^2}\right) \right\}. \tag{A.36}
\end{aligned}$$

References

1. S. Laporta, E. Remiddi, *Phys. Lett.* **B379**, 283 (1996). DOI 10.1016/0370-2693(96)00439-X
2. S.R. Moore, K. Whisnant, B.L. Young, *Phys. Rev.* **D31**, 105 (1985). DOI 10.1103/PhysRevD.31.105
3. F. Jegerlehner, *Acta Phys. Polon.* **B49**, 1157 (2018). DOI 10.5506/APhysPolB.49.1157
4. A. Czarnecki, M. Skrzypek, *Phys. Lett.* **B449**, 354 (1999). DOI 10.1016/S0370-2693(99)00076-3
5. M. Lindner, M. Platscher, F.S. Queiroz, *Phys. Rept.* **731**, 1 (2018). DOI 10.1016/j.physrep.2017.12.001
6. M. Pospelov, A. Ritz, *Annals Phys.* **318**, 119 (2005). DOI 10.1016/j.aop.2005.04.002
7. A. Czarnecki, W.J. Marciano, *Adv. Ser. Direct. High Energy Phys.* **20**, 11 (2009). DOI 10.1142/9789814271844_0002
8. A. Moyotl, A. Rosado, G. Tavares-Velasco, *Phys. Rev.* **D84**, 073010 (2011). DOI 10.1103/PhysRevD.84.073010
9. H. Novales-Sánchez, M. Salinas, J.J. Toscano, O. Vázquez-Hernández, *Phys. Rev.* **D95**(5), 055016 (2017). DOI 10.1103/PhysRevD.95.055016
10. C.F. Chang, P.Q. Hung, C.S. Nugroho, V.Q. Tran, T.C. Yuan, *Nucl. Phys.* **B928**, 21 (2018). DOI 10.1016/j.nuclphysb.2018.01.007
11. V. Keus, N. Koivunen, K. Tuominen, *JHEP* **09**, 059 (2018). DOI 10.1007/JHEP09(2018)059
12. A.I. Hernández-Juárez, A. Moyotl, G. Tavares-Velasco, *Phys. Rev.* **D98**(3), 035040 (2018). DOI 10.1103/PhysRevD.98.035040
13. R. Martínez, M.A. Pérez, N. Poveda, *Eur. Phys. J.* **C53**, 221 (2008). DOI 10.1140/epjc/s10052-007-0457-6
14. R. Gaitan, E.A. Garcés, J.H.M. de Oca, R. Martínez, *Phys. Rev.* **D92**(9), 094025 (2015). DOI 10.1103/PhysRevD.92.094025
15. J.I. Aranda, D. Espinosa-Gómez, J. Montaña, B. Quezadas-Vivian, F. Ramírez-Zavaleta, E.S. Tututi, *Phys. Rev.* **D98**(11), 116003 (2018). DOI 10.1103/PhysRevD.98.116003
16. Q.H. Cao, C.R. Chen, F. Larios, C.P. Yuan, *Phys. Rev.* **D79**, 015004 (2009). DOI 10.1103/PhysRevD.79.015004
17. L. Ding, C.X. Yue, *Commun. Theor. Phys.* **50**, 441 (2008). DOI 10.1088/0253-6102/50/2/32
18. A. Aboubrahim, T. Ibrahim, P. Nath, A. Zorik, *Phys. Rev.* **D92**(3), 035013 (2015). DOI 10.1103/PhysRevD.92.035013
19. R. Martínez, M.A. Pérez, O.A. Sampayo, *Int. J. Mod. Phys.* **A25**, 1061 (2010). DOI 10.1142/S0217751X10048159
20. T. Ibrahim, P. Nath, *Phys. Rev.* **D84**, 015003 (2011). DOI 10.1103/PhysRevD.84.015003
21. V. Khachatryan, et al., *Phys. Rev.* **D93**(5), 052007 (2016). DOI 10.1103/PhysRevD.93.052007
22. A.M. Sirunyan, et al., (2019)
23. A. Czarnecki, B. Krause, *Phys. Rev. Lett.* **78**, 4339 (1997). DOI 10.1103/PhysRevLett.78.4339
24. I.B. Khriplovich, *Phys. Lett.* **B173**, 193 (1986). DOI 10.1016/0370-2693(86)90245-5. [*Yad. Fiz.*44,1019(1986)]
25. E.P. Shabalin, *Sov. J. Nucl. Phys.* **28**, 75 (1978). [*Yad. Fiz.*28,151(1978)]
26. I.D. Choudhury, A. Lahiri, *Mod. Phys. Lett.* **A30**(23), 1550113 (2015). DOI 10.1142/S0217732315501138
27. A.M. Sirunyan, et al., (2019)
28. V. Shtabovenko, R. Mertig, F. Orellana, *Comput. Phys. Commun.* **207**, 432 (2016). DOI 10.1016/j.cpc.2016.06.008
29. H.H. Patel, *Comput. Phys. Commun.* **197**, 276 (2015). DOI 10.1016/j.cpc.2015.08.017
30. Z. Hioki, K. Ohkuma, *Eur. Phys. J. C* **65**, 127 (2010). DOI 10.1140/epjc/s10052-009-1204-y
31. J.F. Kamenik, M. Papucci, A. Weiler, *Phys. Rev. D* **85**, 071501 (2012). DOI 10.1103/PhysRevD.85.071501. [Erratum: *Phys.Rev.D* 88, 039903 (2013)]
32. W. Bernreuther, Z.G. Si, *Phys. Lett. B* **725**, 115 (2013). DOI 10.1016/j.physletb.2013.06.051. [Erratum: *Phys.Lett.B* 744, 413–413 (2015)]
33. S. Larin, J. Vermaseren, *Phys. Lett. B* **303**, 334 (1993). DOI 10.1016/0370-2693(93)91441-O
34. G. Prosperini, M. Raciti, C. Simolo, *Prog. Part. Nucl. Phys.* **58**, 387 (2007). DOI 10.1016/j.pnpnp.2006.09.001
35. M. Tanabashi, et al., *Phys. Rev.* **D98**(3), 030001 (2018). DOI 10.1103/PhysRevD.98.030001
36. T. Hahn, M. Perez-Victoria, *Comput. Phys. Commun.* **118**, 153 (1999). DOI 10.1016/S0010-4655(98)00173-8
37. A. Denner, S. Dittmaier, L. Hofer, *Comput. Phys. Commun.* **212**, 220 (2017). DOI 10.1016/j.cpc.2016.10.013
38. J. Aranda, T. Cisneros-Pérez, J. Montaña, B. Quezadas-Vivian, F. Ramírez-Zavaleta, E. Tututi, (2020)